Quantum Features of a Barely Bound Molecular Dopant: Cs 2 (3 Σ u) in Bosonic Helium Droplets of Variable Size

ARTICLE *in* THE JOURNAL OF PHYSICAL CHEMISTRY A · JUNE 2011

Impact Factor: 2.69 · DOI: 10.1021/jp111825n · Source: PubMed

7 AUTHORS, INCLUDING:

Gerardo Delgado-Barrio
Spanish National Research Council
246 PUBLICATIONS **2,961** CITATIONS
SEE PROFILE

Pablo Villarreal
Spanish National Research Council
202 PUBLICATIONS **2,617** CITATIONS
SEE PROFILE

Franco A Gianturco
Sapienza University of Rome
448 PUBLICATIONS **6,225** CITATIONS
SEE PROFILE

Ersin Yurtsever
Koc University
138 PUBLICATIONS **1,230** CITATIONS
SEE PROFILE

THE JOURNAL OF PHYSICAL CHEMISTRY A

ARTICLE

pubs.acs.org/JPCA

Quantum Features of a Barely Bound Molecular Dopant: $Cs_2(^3\Sigma_u)$ in Bosonic Helium Droplets of Variable Size

Ricardo Pérez de Tudela,[†] David López-Durán,[†] Tomás González-Lezana,[†] Gerardo Delgado-Barrio,[†] Pablo Villarreal,[*,†] Franco A. Gianturco,[‡] and Ersin Yurtsever[§]

[†]Instituto de Física Fundamental, CSIC, Serrano 123, 28006 Madrid, Spain

[‡]Department of Chemistry and CNISM, University of Rome La Sapienza, Piazzale A. Moro 5, 00185 Rome, Italy

[§]Department of Chemistry, Koç University, Rumelifeneri Yolu, 34450 Sariyer, Istanbul, Turkey

ABSTRACT: We present in this work the study of small $^4He_N-Cs_2(^3\Sigma_u)$ aggregates ($2 \le N \le 30$) through combined variational, diffusion Monte Carlo (DMC), and path integral Monte Carlo (PIMC) calculations. The full surface is modeled as an addition of $He-Cs_2$ interactions and He−He potentials. Given the negligible strength and large range of the $He-Cs_2$ interaction as compared with the one for He−He, a propensity of the helium atoms to pack themselves together, leaving outside the molecular dopant is to be expected. DMC calculations determine the onset of helium gathering at $N = 3$. To analyze energetic and structural properties as a function of N, PIMC calculations with no bosonic exchange, i.e., Boltzmann statistics, at low temperatures are carried out. At $T = 0.1$ K, although acceptable one-particle $He-Cs_2$ distributions are obtained, two-particle He−He distributions are not well described, indicating that the proper symmetry should be taken into account. PIMC distributions at $T = 1$ K already compare well with DMC ones and show minor exchange effects, although binding energies are still far from having converged in terms of the number of quantum beads. As N increases, the He−He PIMC pair correlation function shows a clear tendency to coincide with the experimental boson-liquid helium one at that temperature. It supports the picture of a helium droplet which carries the molecular impurity on its surface, as found earlier for other triplet dimers.

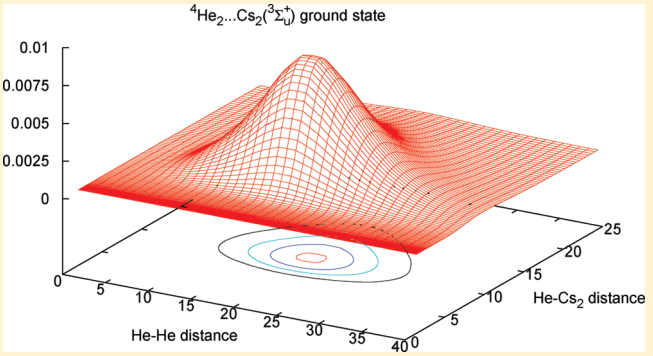

I. INTRODUCTION

The ability to make cold atomic samples that was accessed more than ten years ago has naturally tried to evolve into new areas of interest like the many-body effects and the chemical behavior at ultralow temperatures, although the more complex nature of even the simplest molecules makes to cool and trap them a challenging task. Recent years, however, have witnessed a remarkable increase in our capabilities to produce, observe, and stabilize trapped samples of cold molecules (below 1 K) or of ultracold molecules (below 1 mK).[1−4]

In this largely unexplored temperature regime for molecules, chemical reactions are dominated by tunneling and resonance phenomena that can lead, as an example, to marked increases at specific ultralow temperatures[5] or to a general increase of reaction rates as the temperature decreases.[6] Thus, to develop the ability to trap cold and ultracold molecules for long periods additionally offers an unique environment for high-resolution spectroscopy, for testing the time variations of the fundamental constants, and for exploring parity violation at the molecular level.[7,8]

One common way of generating ultracold, heteronuclear or homonuclear, molecules is to use laser cooled alkali metal atoms by photoassociation or by association on Feshbach resonances,[1] where both polar and nonpolar species are initially produced in excited vibrational states that are then cooled at another stage of the process:[9] in this last example, for instance, a shaped, incoherent broadband diode laser near threshold can be employed to cause selective vibrational population transfer in cold cesium dimers,[9] or more generally optical pumping via femtosecond, mode-locked lasers.[10]

The study of the fundamental properties of molecules, clusters, and molecular complexes at low and very low temperatures can be advantageous for several reasons: on the one hand, the number of accessible molecular states could be reduced by various orders of magnitude, allowing a much less ambiguous assignment process. Furthermore, as mentioned before, specific features of the system like the existence of tiny barriers and of tunneling processes gain importance and may eventually determine the shape of the overall interaction in the system or the evolutions of the processes under study.

The use of He atoms has proven to be a very useful resource in this range of temperatures and within the context of the structural

Special Issue: J. Peter Toennies Festschrift

Received: December 13, 2010
Revised: May 17, 2011
Published: May 17, 2011

studies outlined above: the choice of this inert gas for sympathetic cooling of a broad range of molecules has, in fact, been found to be important since pioneering studies,[11] and the combination of molecular dopants (picked up by a cold cluster of either ^{3}He or ^{4}He atoms as N increases) with spectroscopic analysis,[12,13] has turned out to be a winning arrangement for low-T structural and dynamical studies.[14,15]

Cesium dimer in its triplet ground state $^3\Sigma_u^+$, and in general alkali-metal dimers, play an important role in cold atom−atom/molecule collisions, laser cooling of molecules, and coherent control.[16] In fact, the weakly bound triplet state of alkali dimers is preferentially observed because the energy released when the molecule is formed by atom−atom cold collisions on the surface of the droplet is not sufficient to destroy the system.[14] In this context, visible absorption spectra of cesium-doped cold helium nanodroplets involving the triplet ground state, $^3\Sigma_u^+$, have been reported.[17,18] The latter is the specific electronic state, besides the $^1\Sigma_g^+$ ground state of Cs_2, selected to experimentally investigate the extremely small variations in the electron-to-proton mass ratio,[19] which is considered one of the crucial indicators to validate the models proposed to explain the presence of dark energy in the Universe.

As mentioned above, alkali-metal atoms picked up by a beam of helium nanodroplets move over the droplet's surface where they could meet each other and form molecules in cold collisions, with the latter being expected to remain on that surface. Recent diffusion Monte Carlo (DMC) studies for Li_2 doped ^{4}He clusters indeed reported such a behavior.[20] In the case of Cs_2, the characteristics of the He−He and He−Cs_2 interactions[21] indicate as the more likely the arrangement in which the impurity would be attached to, instead of being immersed into the cluster. In the present work, we analyze to what extent path integral Monte Carlo (PIMC) calculations at low temperatures, within the so-called *primitive* approximation without explicit inclusion of exchange effects, succeed to describe such a challenging scenario for Cs_2 doping ^{4}He clusters which exhibit a very small binding energy and yet a strong angular anisotropy of their interaction.

The next section briefly outlines the main details of the theoretical methods employed in this work, while section III shows the general characteristics of their potential energy surface (PES), the numerical details, and some tests. Section IV presents and analyzes our computational results while the final section V reports our conclusions.

II. THEORETICAL METHODS

A. Variational Treatment. Using satellite coordinates $\{(\mathbf{r}, \mathbf{R}_k)\}$, with $\mathbf{r}$ being the vector for the interparticle distance between the two cesium atoms, and $\mathbf{R}_k$ the vectors from the center of mass of the dimer to the different He atoms, the Hamiltonian which describes the system can be written as[22]

$$H = H^{\mathrm{d}} + \sum_{k=1}^{N} H_k^{\mathrm{t}}(\mathbf{R}_k, r) + \sum_{i<j}^{N} \left[V_{ij}(|\mathbf{R}_i - \mathbf{R}_j|) - \frac{\hbar^2}{2m_{\mathrm{Cs}}} \nabla_i \cdot \nabla_j \right] \quad (1)$$

where H^{d} is the Cs_2 Hamiltonian, and H_k^{t} $(k = 1, N)$ are He−Cs_2 triatomic Hamiltonians containing W, the atom−diatom intermolecular potential, which depends both on the pair of (R_k, r) distances and on the angle θ_k between the $\mathbf{R}_k$ and $\mathbf{r}$ vectors. Finally, eq 1 has a term describing the He−He interactions and a kinetic energy coupling term that has its origin in the use of non-Jacobi coordinates. For a complex containing just a couple of helium atoms, an "exact" variational treatment can be readily applied.[23−26] In the present work, the cesium dimer is kept fixed at its equilibrium distance, i.e., it is considered as a rigid rotor, and consequently, its Hamiltonian, H^{d}, reduces to a rotational term. Moreover, due to the huge mass of cesium, m_{Cs}, a quantum chemistry-like (QC) approach[25,26] is accurate in regard to energy and spatial helium distributions, and such a term can even be neglected. Also, as in the triatomic case, electronic spin effects are taken to be of minor relevance and have been neglected;[21,27] i.e., the cesium dimer has been considered as a pseudo-$^1\Sigma$ partner. Essentially, choosing a body-fixed (BF) frame with the Z^{BF} axis parallel to r, and introducing the quantum numbers associated with the helium orbital angular momentum $\mathbf{l}_k$, ℓ_k, and the He−Cs_2 vibration, n_k, collectively denoted by $\{q_k\} = \{\ell_k n_k\}$, $(k = 1, 2)$, the basis functions are expressed as[23]

$$\Phi^{JK}_{q_1 q_2 L\Omega}(\hat{\mathbf{r}}, \mathbf{R}_1, \mathbf{R}_2) = f_{n_1}(R_1) f_{n_2}(R_2) \mathscr{W}^{JK}_{\ell_1 \ell_2 L\Omega}(\hat{\mathbf{r}}, \hat{\mathbf{R}}_1, \hat{\mathbf{R}}_2) \quad (2)$$

where L is the quantum number associated with the total orbital angular momentum $\mathbf{L} = \mathbf{l}_1 + \mathbf{l}_2$, while the angular functions $\mathscr{W}^{JK}_{\ell_1 \ell_2 L\Omega}$, which depend on the diatomic orientation $\hat{\mathbf{r}} \equiv (\theta_r, \phi_r)$ with respect to a space-fixed reference system, and on the orientations $\hat{\mathbf{R}}_k \equiv (\theta_k, \phi_k)$ in the BF frame can be expressed as combinations of Wigner rotation matrices and spherical harmonics.[26] The f_k are radial functions associated with the He−Cs_2 stretching motion, which are numerically obtained as follows:[26] at different fixed orientations $\{\theta_k\}_{k=1,K}$, one looks for just the ground energy level, w_0, of the Schrödinger equation

$$\left[-\frac{\hbar^2}{2\mu} \frac{\partial^2}{\partial R^2} + W(R, r_{\mathrm{eq}}, \theta_k) - w_0(\theta_k) \right] \phi_0(R; \theta_k) = 0 \quad (3)$$

and the $\phi_0(R; \theta_k)$ eigen-functions are further orthogonalized through a Schmidt procedure, which leads to an orthonormal set of $\{f_k(R)\}_{k=1,K}$ functions. The total wave function is expanded in a symmetry-adapted basis set composed of functions eq 2, which takes into account the relevant symmetry operators of the system, such as the total inversion $\mathscr{E}^*$, the permutation of the He atoms $\mathscr{P}_{12}$, and for a homonuclear dopant, the exchange of diatomic nuclei $\mathscr{P}_{\mathrm{d}}$.[23,24] Finally, the corresponding Hamiltonian matrix is diagonalized by using standard routines[28] or iterative algorithms[29] depending on its size. To gain some insight on the evolution of helium arrangements when the cluster size is changed, the above tetra-atomic model has been extended for systems containing a few more helium atoms, $N > 2$, by considering instead of the Hamiltonian of eq 1, the following effective Hamiltonian:

$$H^{\mathrm{eff}} = H^{\mathrm{d}} + \frac{N}{2} \sum_{k=1}^{2} H_k^{\mathrm{t}}(\mathbf{R}_k, r) + \frac{N(N-1)}{2} \tilde{V}_{12} \quad (4)$$

which essentially accounts for N triatomics grouped into $N/2$ identical tetra-atomics and $\binom{N}{2}$ identical, $\tilde{V}_{12}$, He−He interactions. Note that this term increases quadratically with the number of helium atoms while the former does it linearly.

B. Diffusion Monte Carlo Treatment. The DMC treatment has been already described elsewhere.[21,30,31] We adopted the QC approach; i.e., the rotation of the cesium dimer was completely neglected. The total trial wave function of the system containing

N helium atoms is expressed as the product of purely nodeless exponential forms:[32]

$$\Psi_T = \prod_{i=1}^{N} \varphi_{He-Cs_2}(\mathbf{R}_i) \prod_{i<j} \Psi_{He-He}(|\mathbf{R}_i - \mathbf{R}_j|) \quad (5)$$

with

$$\begin{aligned}\varphi_{He-Cs_2}(\mathbf{R}_i) &= \varphi_{He-Cs_2}(R_i,\cos\theta_i)\\ &= \exp(f_0^{He-Cs_2}(R_i)[P_0(\cos\theta_i)+1]\\ &+ \sum_{n=1}^{n_{max}} \{f_{2n}^{He-Cs_2}(R_i)[P_{2n}(\cos\theta_i)+1]\\ &+ f_{-2n}^{He-Cs_2}(R_i)[-P_{2n}(\cos\theta_i)+1]\})\end{aligned} \quad (6)$$

where the homonuclear character of the Cs_2 molecule is taken into account through the parity of the Legendre polynomials P_k, and $f_k^{He-Cs_2}(R)$ are Jastrow functions:

$$f_k^{He-Cs_2}(R) = -\left(\frac{p_5}{R^5}+\frac{p_3}{R^3}+\frac{p_2}{R^2}+p_1R+p_0\ln R\right) \quad (7)$$

In fact, the φ_{He-Cs_2} trial function was fitted to the one coming from the tetra-atomic variational calculation.

The helium−helium part of the wave function is the product of functions:

$$\Psi_{He-He}(|\mathbf{R}_i - \mathbf{R}_j|) = \exp\{f^{He-He}(|\mathbf{R}_i - \mathbf{R}_j|)\} \quad (8)$$

where the functional form of f^{He-He} is the same as f^{He-Cs_2} for $N > 3$, while for $N = 2$, 3 we found adequate a similar but somewhat different expression,

$$f^{He-He}(R) = -\left[\sum_{k=0}^{2}\frac{p_{2k+1}}{R^{2k+1}} + \sum_{k=1}^{3} q_{2k+1}(R-R_0)^{2k+1}\right] \quad (9)$$

In other words, the He−He trial function was adapted to the cluster size under study: for $N = 2$ and 3, eq 9 was fitted to the results coming from variational calculations, while for larger clusters we considered the Jastrow-type functions corresponding to pure helium clusters.[33] Note that the boson character of the total trial wave function, eq 5, is not modified along the DMC process.[34]

C. Path integral Monte Carlo Approach. The PIMC approach for the calculation of the thermodynamical properties of quantum systems at a finite temperature has been described elsewhere.[35] All the properties of the system can be extracted from the partition function:

$$Z = \int d\mathscr{R}\, \rho(\mathscr{R},\mathscr{R};\beta) \quad (10)$$

where $\beta = 1/k_BT$ and k_B is the Boltzmann constant, $\mathscr{R}$ is a vector collecting the Cartesian coordinates of the particles of the system and ρ, the density matrix at a given temperature T, can be factorized in $\mathbf{M}$ matrices at a temperature MT, as follows:

$$\rho(\mathscr{R}_0,\mathscr{R}_M;\beta) = \int d\mathscr{R}_1 \ldots d\mathscr{R}_{M-1} \prod_{\alpha=1}^{M} \rho(\mathscr{R}_{\alpha-1},\mathscr{R}_\alpha;\tau) \quad (11)$$

where $\tau = \beta/M$. The M number defines the *beads* that constitute each *polymer* or a quantum path.[35] These new *hot* density operators can be factorized using the identity:[36]

$$\begin{aligned}\hat{\rho} &= e^{-\tau(\hat{\mathscr{T}}+\hat{\mathscr{V}})}\\ &= e^{-\tau\hat{\mathscr{T}}}e^{-\tau\hat{\mathscr{V}}}\exp\left\{\frac{\tau^2}{2}[\hat{\mathscr{V}},\hat{\mathscr{T}}] - \frac{\tau^3}{6}[\hat{\mathscr{V}},[\hat{\mathscr{V}},\hat{\mathscr{T}}]] + \ldots\right\}\end{aligned} \quad (12)$$

As $\tau \to 0$ the terms containing the commutators can be neglected, a choice known as the *primitive approximation*. There are, however, numerous works that go beyond this first-order approximation and include higher order terms in the expansion of the density operator in eq 12.[37,38] In these approaches the number of beads, M, needed to fully describe the quantum nature of the system is drastically reduced, with the drawback of additionally having to evaluate potential derivatives. The final expression for the density function under the primitive approximation becomes

$$\rho(\mathscr{R}_0,\mathscr{R}_M;\beta) = \left(\frac{1}{4\pi\lambda\tau}\right)^{-3NM/2}\int d\mathscr{R}_1 \ldots d\mathscr{R}_{M-1} \times \exp\left[-\tau\sum_{m=1}^{M}\frac{m}{2\tau^2}(\mathscr{R}_{m-1}-\mathscr{R}_m)^2 - \tau V(\mathscr{R}_m)\right] \quad (13)$$

where $\mathscr{R}_\alpha$ is the vector which collects the Cartesian positions of the N particles: $\mathscr{R}_\alpha \equiv \{\mathbf{R}_1^\alpha, \ldots, \mathbf{R}_N^\alpha\}$, being $\mathbf{R}_i^\alpha$ the position vector of the ith He atom at the time *slice* or *imaginary* time α, and $\lambda = \hbar^2/2m$.

For the computation of the internal energy of the system, basically two estimators have been developed.[39] In this work, we have used the *virial estimator*,[40] which states that the kinetic energy is proportional to the scalar product of position and potential gradients:

$$E_v = \frac{3}{2}Nk_BT + \left\langle \frac{1}{2M}\sum_{\alpha=1}^{M}\sum_{i=1}^{N}(\mathbf{R}_i^\alpha - \overline{\mathbf{R}}_i)\cdot\frac{\partial V(\mathbf{R}_i^\alpha)}{\partial \mathbf{R}_i^\alpha} + \frac{1}{M}\sum_{\alpha=1}^{M} V(\mathscr{R}_\alpha)\right\rangle_{MC} \quad (14)$$

where $\overline{\mathbf{R}}_i$ is the *centroid* of the particle i and is given as $\overline{\mathbf{R}}_i = M^{-1}\sum_{\alpha=1}^{M}\mathbf{R}_i^\alpha$, and the brackets indicate average over Monte Carlo (MC) steps. The virial kinetic energy estimator is expressed as the classical term proportional to T plus a quantum correction. This estimator is considered as more accurate than other choice, the *thermodynamic estimator*,[41] which does not need the derivatives of the potential. Note that the specific case $M = 1$ corresponds to the classical description of the system.[42] Finally, the integration is carried out via MC as an average over a number of cyclic paths $\{\mathscr{R}_0, \mathscr{R}_1, \ldots, \mathscr{R}_{M-1}, \mathscr{R}_M = \mathscr{R}_0\}$ sampled according to a probability density proportional to the factorized product of $\mathbf{M}$ density matrices of eq 11. As with QC and DMC, PIMC calculations have been performed considering the dopant as a nonrotating rigid body.

The present study includes the analysis of the various one- and two-particle properties, i.e., angular and radial distributions of the individual He atoms estimated as

$$\mathscr{D}_N(\cos\theta) = \frac{1}{NM}\left\langle\sum_{\alpha=1}^{M}\sum_{k=1}^{N}\delta(\cos\theta - \cos\theta_k^\alpha)\right\rangle_{MC} \quad (15)$$

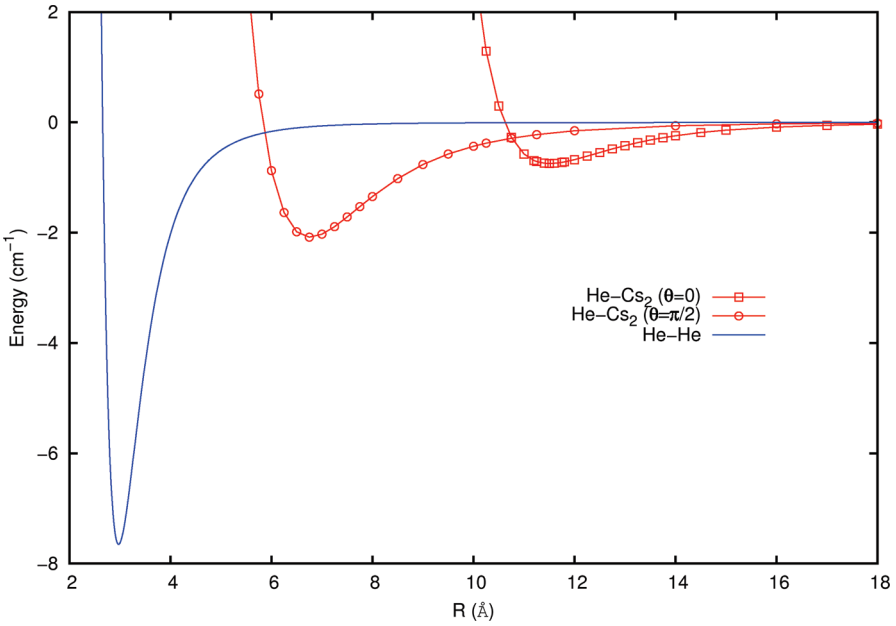

Figure 1. He−He potential and He−Cs_2 interaction at the two extreme configurations $\theta = 0, \pi/2$.

and

$$\mathscr{D}_N(\mathrm{R}) = \frac{1}{NM}\left\langle \sum_{\alpha=1}^{M}\sum_{k=1}^{N} \delta(\mathrm{R} - |\mathbf{R}_k^\alpha|) \right\rangle_{\mathrm{MC}} \quad (16)$$

respectively, as well as angular distributions of cos γ, γ being the angle formed by any couple of vectors $\mathbf{R}_k$, $\mathbf{R}_l$ $(k \neq l)$ joining the corresponding He atoms and the center of mass of the cesium dimer, which is calculated as

$$\mathscr{D}_N(\cos\gamma) = \frac{2}{N(N-1)M}\left\langle \sum_{\alpha=1}^{M}\sum_{k<l}^{N} \delta(\cos\gamma - \hat{\mathbf{R}}_k^\alpha \cdot \hat{\mathbf{R}}_l^\alpha) \right\rangle_{\mathrm{MC}} \quad (17)$$

where $\hat{\mathbf{R}}_k^\alpha = \mathbf{R}_k^\alpha/\mathrm{R}_k^\alpha$, and pair He−He distance distributions:

$$\mathscr{D}_N(\mathrm{R}_{\mathrm{He-He}}) = \frac{2}{N(N-1)M}\left\langle \sum_{\alpha=1}^{M}\sum_{k<l}^{N} \delta(R_{\mathrm{He-He}} - |\mathbf{R}_k^\alpha - \mathbf{R}_l^\alpha|) \right\rangle_{\mathrm{MC}} \quad (18)$$

A commonly used magnitude to describe the structure of liquids is the pair-correlation function, $g(r)$. For boson-liquid helium, it has been experimentally determined at low temperatures through neutron-diffraction[43] and X-ray scattering[44] measurements. For clusters, a size-dependent helium−helium pair-correlation can be defined from the above pair distance distributions, eq 18, as

$$g_N(\mathrm{R}_{\mathrm{He-He}}) \propto N\mathscr{D}_N(\mathrm{R}_{\mathrm{He-He}})/\mathrm{R}_{\mathrm{He-He}}{}^2 \quad (19)$$

which allows us to study the evolution of helium arrangements within doped clusters.

D. Evolutionary Algorithm. It is convenient for a PIMC calculation to have the classical equilibrium configuration of the system as the starting point of its propagation. For clusters with low dimensionality, classical MC is sufficient to achieve this goal. However, as the dimensionality of the system increases, the problem of finding the global minimum of the PES becomes gradually harder. Evolutionary algorithms have proven to be helpful to this end,[45] mimicking the way natural species evolve from generation to generation.

In a similar way as natural selection and competition among animal species evolve, we have implemented a specific version of an evolutionary algorithm.[46] Here, each individual i is associated to a specific cluster, so it has assigned a vector x_i containing the Cartesian coordinates of all its atoms. This vector has $n = 3N$ dimensions, N being the number of atoms in the cluster. The algorithm follows the usual procedure of initialization with a random solution to the problem (thus defining the father), mutation (with slight random changes in the coordinates of the new children), struggle (with the competition of random opponents within the group of father and children), and selection (which generates the new parents for the next iteration). This process is repeated until the optimal solution is eventually reached.

III. POTENTIAL ENERGY SURFACE AND NUMERICAL DETAILS

A. Potential Energy Surface. As it is commonly used in this type of system, and already tested over several helium cluster−dimer complexes,[47,48] the PES representing the interaction of N helium atoms and one cesium dimer, frozen at its equilibrium distance r_{eq}, can be accurately described as an addition of N He−Cs_2 triatomic potentials plus $N(N + 1)/2$ He−He pair interactions. Using satellite coordinates, this is written as

$$V = \sum_{k=1}^{N} W(R_k, r_{\mathrm{eq}}, \theta_k) + \sum_{k=1}^{N}\sum_{k'\neq k} V_{kk'}(|\mathbf{R}_k - \mathbf{R}_{k'}|) \quad (20)$$

where the triatomic interactions, W, are analytical anisotropic Lennard-Jones potential forms, fitted to ab initio points,[21] while each helium pair interaction, $V_{kk'}$, is also analytically represented by a Tang−Toennies potential.[49] As mentioned above, an accurate, fully analytical representation of the PES is of crucial importance not only to speed up PIMC calculations but also to

reach confident results through the virial estimator of the kinetic energy that involves potential derivatives. Figure 1 displays the extreme (T-shaped and collinear) He−Cs_2 interactions, together with the He−He one, both terms driving the behavior of He_N−Cs_2 aggregates. All interactions are very weak, although it is clear the larger strength of the helium-pair interaction over the helium−cesium one, independently of its angular arrangement: its well depth is about 4 times that of the T-shaped He−Cs_2 potential, and its location is at much shorter distances than the latter. Therefore, although the mass effect leads, for isolated species, to a binding energy of only ∼0.0009 cm^{-1} for the ^{4}He dimer,[33,50,51] the rotation-less He−$Cs_2(^3\Sigma)$ bound state is only at −0.10 cm^{-1},[21] and we shall see a tendency of the He atoms to get closer to each other with increasing cluster size and to push the cesium dimer outside what tends to become a pure helium cluster.

B. Numerical Details. In the calculations presented here the following masses (amu) were used: m_{Cs} = 132.90545, $m_{^4He}$ = 4.00260. The Cs_2 molecule was kept at its equilibrium distance r_{eq} = 6.8 Å.

For variational calculations, a grid of 8192 points in the R range 2−200 Å was employed to solve numerically eq 3 using a Numerov procedure. Eight equally spaced values of θ_k in the interval $[0, 4\pi/9]$ were included. To speed up the numerical radial quadratures, an interpolation of 1000 Gaussian points in the above-mentioned R range was performed for the $\{f_k\}$ functions. Expansions of the He−He and He−Cs_2 analytical interactions in Legendre polynomials were carried out by considering 101 Gauss-Legendre points in the $[0, \pi]$ interval. To avoid spurious results, a cutoff of 5000 cm^{-1} was imposed on the two interactions. At a total angular momentum J = 0, and even values of the inversion parity, the exchange of He atoms, and the permutation of Cs atoms, energy convergence was achieved to within 10^{-2} cm^{-1} by using even L values up to 14 and $15 \nearrow_i$, (i = 1,2), values, i.e., $0 \le \nearrow_i \le 14$.

For DMC calculations the He−Cs_2 trial function was fitted to the one coming from the N = 2 variational calculations, and its parameters are listed in Table 1. The He−He trial function was determined depending on the cluster size. For N = 2 and 3, eq 9 was fitted to the variational results obtained by using the Hamiltonian eq 4 to solve the associated Schrödinger equation. Table 2 collects the corresponding parameters. For larger clusters, we considered Jastrow-type functions corresponding to pure helium clusters[33] whose parameters are listed in Table 1 of that reference. Diffusion simulations were carried out[21] by using 2000 walkers, a time step τ = 300 hartree^{-1}, parameters w_{min} = 0.5 and w_{max} = 2 controlling the variable population of walkers, and α = 1 for updating the reference energy. Finally, the imaginary-time simulation up to a total time of 3.7 × 10^8 hartree^{-1} was divided in 50 blocks.

Table 3 collects the energy minima of the PES for different sizes of pure (second column) and Cs_2 doped helium clusters (third column), together with their difference as a measure of the contribution due to the impurity (fourth column) which, in addition, is shown as percentage in the fifth column. They were obtained via the evolutionary algorithm described in the main text. Note the excellent agreement with the results from simulated annealing,[33] see Table 3 in that reference. It is clear the dominance of the He−He interactions over the impurity-He ones, which increases quickly with increasing N, the latter amounting only ∼2% for the biggest cluster studied.

For the tetra-atomic cluster (N = 2), we have performed a convergence study on the number of beads for a temperature of 0.1 K. In Table 4 one can see that M = 500 beads are already enough to describe the quantum nature of the system, although at so low temperature exchange effects become very important as it will be shown below. Beyond that value of M, and in spite of the fact that potential $\langle K_v \rangle$ and kinetic $\langle K_v \rangle$ terms display an oscillatory behavior, no significant changes in the energy $\langle E_v \rangle$, which is kept within 0.03 cm^{-1}, are observed.

Table 1. Parameters in Atomic Units of the He−Cs_2 Trial Function[a]

	p_0	p_1	p_2	p_3	p_5
p_0	0.5	0	1	1500	0
p_2	0.5	0.01	1	100	0
p_{-2}	0.5	0	1	100	0

[a] Here[32,52] p_{-2} means $-p_2$.

Table 2. Parameters in Atomic Units of the He−He Trial Function for N = 2, 3, eq 9′[a]

N	R_0	p_1	p_3	p_5	q_1	q_3	q_5	q_7
2	196.00	3.660	−1.763	0	−0.09	6.65 (−6)	−1.39 (−10)	0
3	−453.18	10.404	−0.529	0.011	−0.008	2.72 (−8)	−1.41 (−15)	2.99 (−19)

[a] Numbers in parentheses are powers of ten.

Table 3. Energies of the PES Global Minima of the Complexes He_N and Cs_2He_N, in the Second and Third Columns, Respectively, for $N \le 30$ (cm^{-1}), Computed via the Present Evolutionary Code, and the Corresponding Difference in Absolute and Percentage Values, in the Fourth and Fifth Columns, Respectively

N	$V_{min}(He_N)$	$V_{min}(Cs_2He_N)$	ΔV_{min}	%
1		−2.08	−2.08	100
2	−7.62	−11.89	−4.17	36
4	−45.75	−52.61	−6.86	13
6	−96.07	−103.90	−7.83	8
8	−149.68	−160.28	−10.60	7
10	−213.91	−225.19	−11.28	6
20	−574.37	−590.54	−16.17	3
30	−925.47	−943.74	−18.27	2

Table 4. Bead Convergence Study on Cs_2He_2 (cm^{-1})

M	$\langle V \rangle$	$\langle K_v \rangle$	$\langle E_v \rangle$
1	−11.55	0.21	−11.34
100	−3.88	1.70	−2.18
200	−2.50	1.46	−1.04
300	−2.05	1.32	−0.74
500	−1.50	1.07	−0.43
1000	−1.64	1.23	−0.42
1500	−1.61	1.16	−0.45
2000	−1.73	1.31	−0.42

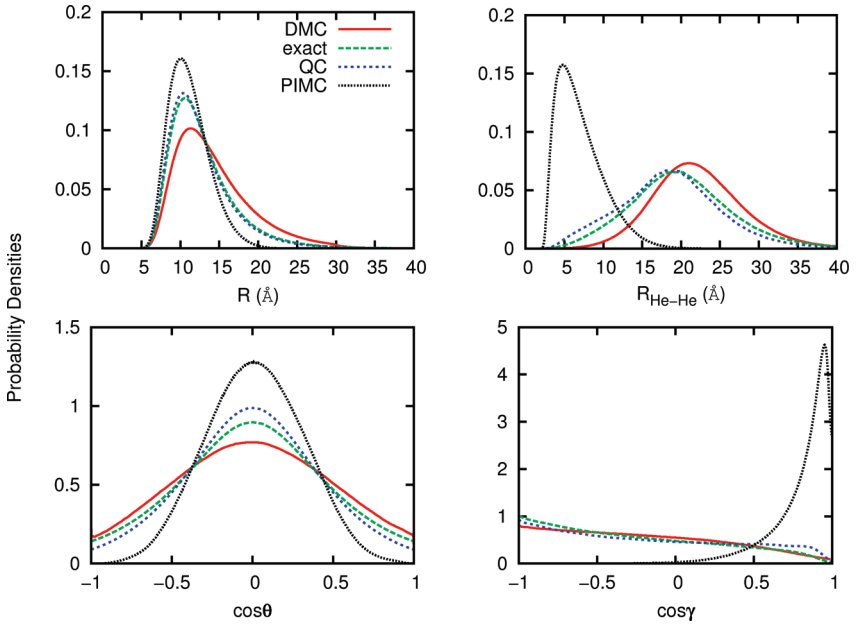

Figure 2. Probability distributions for $N = 2$ from variational calculations including (exact) or not (QC) the cesium dimer rotation, DMC, and PIMC ($T = 0.1$ K) ones. See text.

For larger clusters ($N = 6, 8, 10, 30$) we have performed PIMC calculations at 1 K, a value of the temperature at which experimental determination of boson-liquid helium pair correlation function has been carried out.[43] Increasing temperature allows us to reduce the number of beads in our calculations. Following the general trend $M \propto T^{-1}$, $M \sim 50$ should be enough for $T = 1$ K: our choice was $M = 64$. The probability for the particles to evaporate increases with temperature, and therefore, for that reason, a confinement scheme has been used in systems with more than five He atoms. We define a helium droplet confinement radius of $R_c = 15$ Å and, furthermore, a maximum distance of any atom to the center of mass of Cs_2 to be $R_{max} = 30$ Å. Such restrictions have been chosen to be small enough to avoid evaporation and at the same time large enough to essentially not affect the results. Due to the high value of M, smart collective movements of the beads become mandatory. We have chosen the *staging* sampling method,[53] which samples the kinetic part of the action exactly, while a Metropolis[54] algorithm is applied to the potential part. Within this strategy, thermalization is reached in a reasonable number of MC steps. A total of 10^7 MC steps was carried out in each run after another 10^7 steps for thermalization. The errors were computed using the standard blocking procedure for correlated data.[39]

IV. RESULTS

For $N = 2$, Figure 2 compares the different distributions obtained from DMC, exact variational ($J = 0$), QC (neglecting dimer cesium rotation), and PIMC ($T = 0.1$ K, $M = 500$, no confinements) calculations. It is worth noticing that exact variational and QC results are essentially the same, thus supporting the negligible contribution of the dopant rotation. The two panels on the left refer to one-particle distributions, i.e., the radial distribution (upper panel) in terms of the distance from any of the helium atoms to the cesium dimer center of mass and the angular distribution (lower panel) showing its orientation with respect to the dimer axis. The two panels on the right show two-particle distributions: that of the He−He distance (upper panel) and that of the He−Cs_2-He γ angle. The first three methods lead, although with small differences, to similar results for all the four distributions. The PIMC approach, in turn, produces narrower but alike one-particle distributions: the helium atoms are slightly closer to the dimer and placed more markedly in a perpendicular orientation with respect to the cesium axis. The main discrepancy, however, is exhibited by the two-particle distributions. Regarding helium−helium distances, PIMC produces a distribution that peaks at ∼5 Å and extends not beyond ∼20 Å; i.e., it is placed inside the He−He potential well. On the contrary, DMC, exact, and QC methods predict broader distributions with a maximum at ∼20 Å ranging from ∼5 Å up to ∼40 Å, the He atoms being very far from each other. Accordingly, for the γ angle, while DMC, exact and QC results remain close to each other and show a rather isotropic distribution, although with a tendency of the He atoms to be well separated, PIMC shows a packing of them. The corresponding binding energies in cm^{-1}, 0.174 ± 0.017 (DMC), 0.2041 (exact), and 0.2085 (QC), although with differences, compare acceptably well among them. On the contrary, PIMC produces a value of 0.42 ± 0.06, which looks suspicious. The disagreement between PIMC results and those obtained by variational and DMC calculations, and in particular that related to two-particle distributions, is indeed due to exchange symmetry effects of He atoms which at 0.1 K become important and are not included in our PIMC code. In fact, the thermal wavelength $\Lambda(T) = (2\pi\hbar^2/mk_BT)^{1/2}$ for boson He at $T = 0.1$ K is of ∼27.5 Å, almost 1 order of magnitude longer than the He−He equilibrium distance.

Thus, Boltzmann PIMC predicts a premature gathering of He atoms at $N = 2$. DMC calculations have been performed to determine the crossover size at which this effect actually occurs. For $N = 3$, Figure 3 displays DMC probability densities as in Figure 2. Also model distributions, obtained by solving variationally the Schrödinger equation with the effective Hamiltonian eq 4, are depicted. This model allowed us to estimate the

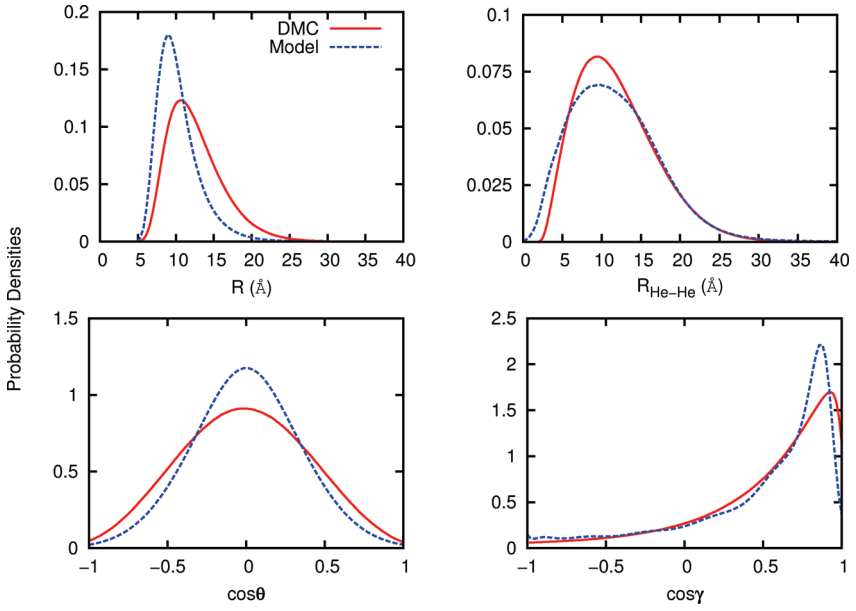

Figure 3. Probability distributions for $N = 3$ from DMC calculations and model variational ones using an efective Hamiltonian, eq 4.

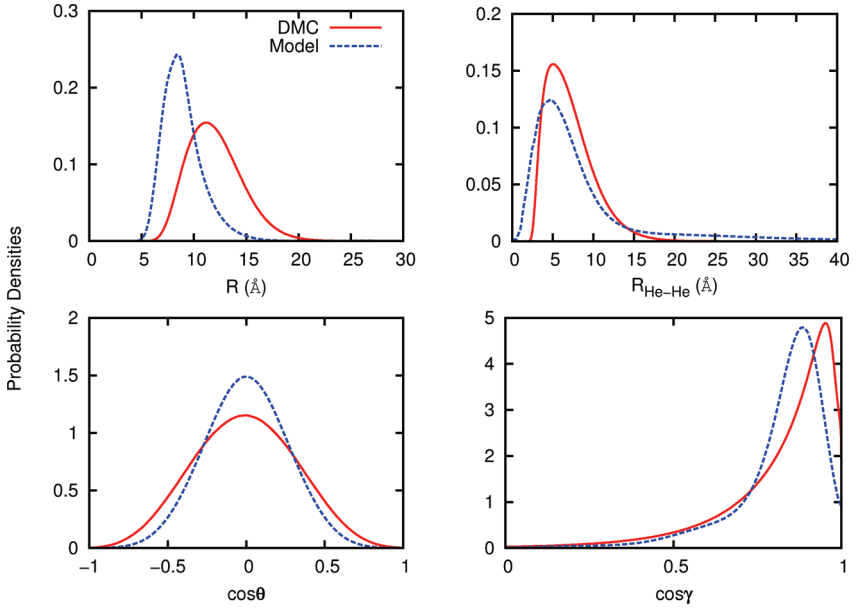

Figure 4. Same that Figure 3 for $N = 4$.

trial He−He function for the DMC calculations as mentioned above. As can be seen, one-particle DMC and model distributions are similar and show that the He atoms are placed around 10 Å from the Cs_2 center of mass, preferably in a perpendicular orientation with respect to the dimer axis. Two-particle distributions, although with differences, behave alike and clearly manifest that at $N = 3$ the helium atoms already prefer to be packed outside the dopant. So, the He−He distance peaks at ∼10 Å (to be compared with the peak exhibited for $N = 2$ at ∼20 Å) and extends up to 30 Å. Accordingly, the cos γ distributions, although covering the whole range, show acute maxima close to cos γ = 0.9. The binding energies obtained trough the two calculations are in very good agreement: 0.420 ± 0.021 cm^{-1} (DMC) vs 0.424 cm^{-1} (model).

To analyze the gradual change of the various distributions in terms of the cluster size, DMC calculations have also been performed for $N = 4$. The trial He−Cs_2 function was, as in the precedent case, the one coming from the variational He_2−Cs_2 calculation, while for the He−He distance we considered a Jastrow-type function corresponding to the pure helium cluster of that size.[33] The results, depicted in Figure 4, are compared with those produced by the crude variational model. The diverse DMC distributions describe a clear picture of the cluster: the helium atoms are mainly located in a perpendicular orientation with respect to the cesium dimer axis at a distance near 10 Å. The distance between two He atoms peaks now at ∼5 Å and extends up to ∼20, Å, being more confined than the corresponding distribution for $N = 3$. Also, the preferred He−He distance is

dx.doi.org/10.1021/jp111825n |J. Phys. Chem. A 2011, 115, 6892–6902

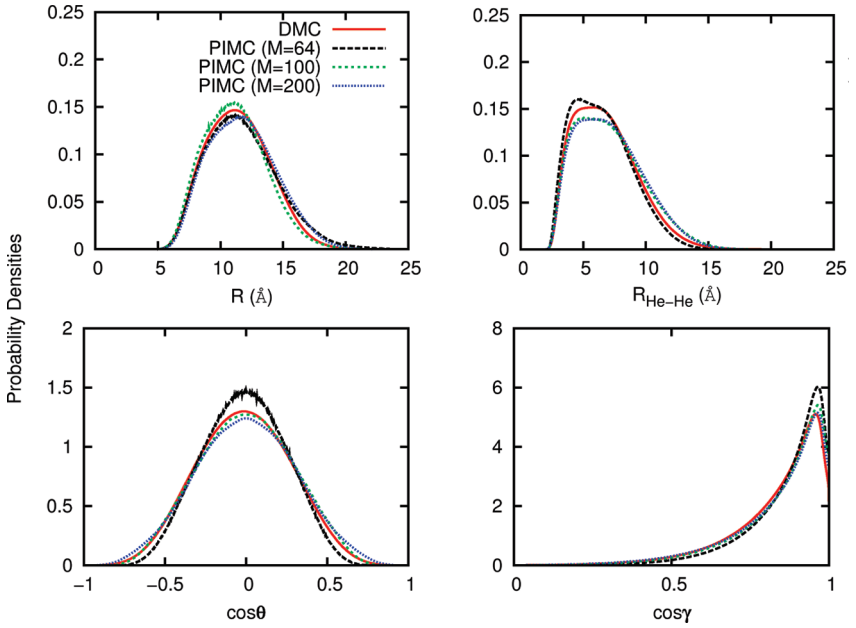

Figure 5. PIMC (T = 1 K) probability distributions for N = 10 in terms of the number of beads, M, and corresponding DMC results.

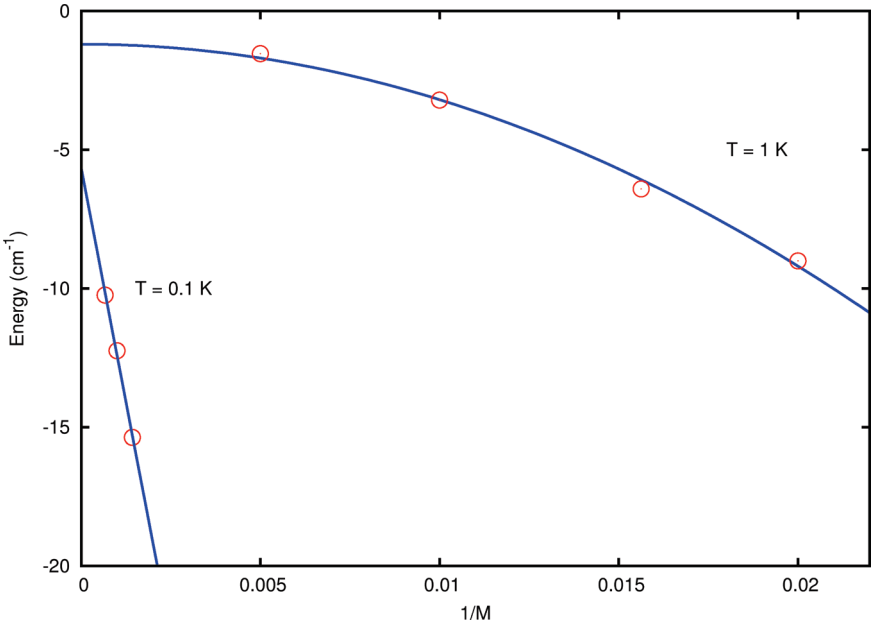

Figure 6. For N = 10, study of energy convergence in terms of $1/M$.

shorter than the He−Cs_2 distance. Thus, the helium atoms form a well separated cluster from the dopant. Again, the DMC and model distributions, although with evident differences, show a qualitative agreement. As a matter of fact, the binding energies yielded by the two calculations are in a reasonable agreement: 1.354 ± 0.016 cm^{-1} (DMC), to be compared with 1.418 cm^{-1} (model).

Larger clusters, $6 \leq N \leq 30$, have been studied through PIMC at T = 1 K, for which the thermal wavelength is drastically reduced ($\Lambda \sim 8.7$ Å) becoming comparable and not much larger than the He−He equilibrium distance. Hence, exchange can be expected to show minor effects, in particular on the structural properties considered here, as occurs for condensed helium[35] at T = 2 K, or para-hydrogen clusters[55] at T = 1.5 K. In addition, the clusters behave in a more classic manner as the size increases and accordingly the number M of beads to get reliable quantum results could in principle be reduced. As mentioned above, we have considered M = 64. For $N \geq 6$, the different distributions obtained through PIMC have similar characteristics. So, radial He−Cs_2 distributions present a unique peak located at ∼10 Å for N = 6, which moves outward with increasing size up to ∼12 Å, extending up to 25−30 Å. In turn, the distributions of the angle θ show a confinement of He atoms in perpendicular orientation with respect to the dopant, while the corresponding distributions

dx.doi.org/10.1021/jp111825n |J. Phys. Chem. A 2011, 115, 6892–6902

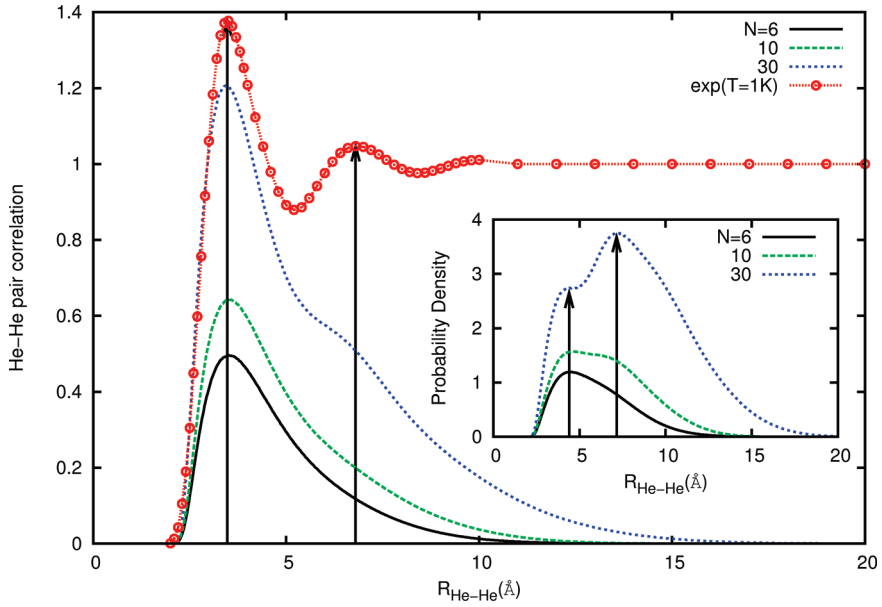

Figure 7. PIMC evolution of the pair correlation function with the cluster size at T = 1 K. They come from the corresponding He−He distance distributions, normalized to N, shown in the inset. Experimental[43] results for boson-liquid helium at the same temperature are also depicted.

for the angle γ present their maximum near cos γ = 1, indicating that the He atoms remain packed themselves. A gradual spreading of the two angular distributions is observed with increasing N.

To realize to what extent M = 64 is sufficient, for N = 10, we have carried out additional PIMC calculations using M = 100 and 200. Figure 5 depicts the various one- and two-particle distributions obtained from those calculations, and compares them with DMC results: all of them are pretty close. Hence, exchange plays a minor role and Boltzmann PIMC results become reliable at this temperature. Eventually, only small differences can be seen among the various PIMC results. The He−He distance distribution exhibits, for M = 64, a small peak at 5 Å while for larger M the distributions show a plateau at 5−7 Å. Note the reduction of this preferred distance from the case N = 3. Also, the M = 64 angular distributions are slightly more pronounced and confined around $\theta = \pi/2$ and near γ = 0 than those coming from larger M. Hence, we consider that PIMC calculations (T = 1 K) for M = 64 are realistically describing the actual structural features of the systems under study.

This is not the case with binding energies: for N = 10, we have investigated the behavior of the energy in terms of $1/M$ and the results of such PIMC calculations for T = 1 K are shown in Figure 6. They show a rather strong variation which goes from −9 at M = 50 to −1.5 cm^{-1} at M = 200. In a similar way to what was done for the LiH−^{4}He cluster,[56] the energies were fitted to a quadratic expression $-E_b + c/M^2$, leading to a binding energy E_b = 1.19 cm^{-1}. Taking into account the (T = 0 K) DMC result of 8.65 cm^{-1},[57] which when compared with the value reported[33] for the pure helium cluster of 5.91 cm^{-1}, guarantees the attachment of the cesium dimer to the helium droplet, one sees that the effect of temperature on the binding energy of the system is much more profound than what in principle would be expected. The present result, however, is completely in accord to recent PIMC studies on pure He_N clusters[58] which also show strong variations of energies for temperatures over 0.75 K. Despite the deficiencies coming from the lack of exchange effects, a similar study has been performed at T = 0.1 K. Values of the corresponding energies obtained with the PIMC method as a function of $1/M$ are included for comparison in Figure 6. A linear fitting yields a binding energy of ∼5.6 cm^{-1} as an extrapolated value for $M \rightarrow \infty$, which is certainly closer to the T = 0 K DMC result than the above-discussed situation for T = 1 K. Due to the use of the primitive approximation, a prohibitive large M value is required, and a proper convergence is not achieved. Hence, we decided not to include PIMC energy estimations in the present study.

An important issue concerns the pair correlation functions $g_N(R_{He-He})$, eq 19. Figure 7 depicts their evolution with the number of He atoms. They were obtained from the corresponding pair He−He distributions, normalized to N, which are shown in the inset. From N = 6, where there is a peak near 4.5 Å, the signature of a secondary peak around 7 Å does appear at N = 10, becoming the maximum at N = 30. This shows the coexistence of two dominant He−He distances in the clusters of this size, which are packed and outside the dopant molecule. In Figure 7 we also display the pair correlation function[43] of boson-liquid helium obtained at the same temperature of 1 K by using neutron diffraction techniques. PIMC computed g-functions indeed show a clear tendency to match the experimental structure: the main peak at 3.5 Å is perfectly reproduced already from small clusters (N = 6), and even the secondary peak becomes evident by the presence of a marked shoulder at 6.8 Å, for N = 30. Thus, the helium atoms tend to pack themselves forming almost pure clusters and their structure remains unaltered by the presence of the dopant, which is placed outside.

V. CONCLUSIONS

Using variational and DMC methodologies, together with finite temperature ones (PIMC), we have tackled the study of extremely weakly bound He_N−$Cs_2(^3\Sigma)$ complexes. To simplify the problem, the rotation of the dopant (rotational constant ∼5.5 × 10^{-3} cm^{-1}) was neglected in DMC and PIMC calculations. The PES was described as a sum of He−Cs_2 interactions

plus the He−He interactions, the cesium dimer bond being frozen at its equilibrium value. Classically, due to the characteristics of the PES, the helium atoms would be packed leaving the dopant outside. Actually, variational and DMC quantum calculations show that this is the situation for clusters containing at least three helium atoms. Boltzmann PIMC calculations within the primitive approximation have been carried out at low temperatures. They show that exchange effects are important at $T = 0.1$ K and should be taken into account. However, these effects play a minor role at $T = 1$ K and can be neglected. The calculations predict a structure in which the cesium dimer sits outside the He droplet as in the lithium case.[20] Such structure is further confirmed through the evolution of the pair correlation helium−helium function which nicely tends with increasing size to the experimental one corresponding to boson-liquid helium.

Within the primitive approximation, however, convergence of binding energies is still hard to achieve in terms of the number of quantum beads, and extrapolation techniques are required to get approximate values. Hence, inclusion of higher order terms in the expansion of the density operator becomes mandatory. Also, we plan a further analysis of these aggregates using quantum chemistry type calculations at the Hartree/Hartree−Fock level,[22,59,60] and more accurate methods as configuration-interaction nuclear orbital approaches for doped boson[61] or fermion[62] helium clusters. Work in these directions is currently in progress.

AUTHOR INFORMATION

Corresponding Author
*E-mail: p.villarreal@iff.csic.es.

ACKNOWLEDGMENT

We thank the Centro de Cálculo (IFF), CTI (CSIC), and Centro de Supercomputación de Galicia (CESGA) for allocation of computer time. This work has been supported by by DGICYT, Spain, Grant Nos. FIS2007-62006 and FIS2010-18132. The computational support of the HPC Consortium CASPUR (Rome) is also acknowledged.

REFERENCES

(1) Dulieu, O.; Gabbanini, C. *Rep. Prog. Phys.* **2009**, *72*, 086401.
(2) Doyle, J.; Friedrich, B.; Krems, R. V.; Masnou-Seeuws, F. *Eur. Phys. J. D* **2004**, *31*, 149.
(3) Julienne, P. S. *Nature* **2003**, *24*, 424.
(4) Barletta, P.; Tennyson, J.; Baker, P. F. *N. J. Phys.* **2009**, *11*, 055029.
(5) Bodo, E.; Gianturco, F. A.; Balakrishnan, N.; Dalgarno, A. *J. Phys. B* **2004**, *37*, 3641.
(6) Bodo, E.; Gianturco, F. A. *Eur. Phys. J. D* **2004**, *31*, 423.
(7) Hudson, E. R.; Lewandowski, H. J.; Sawyer, B. C.; Ye, J. *Phys. Rev. Lett.* **2006**, *96*, 143004.
(8) Bast, R.; Schwerdtfeger, P. *Phys. Rev. Lett.* **2003**, *91*, 23001.
(9) Sofikitis, D.; Horchani, R.; Li, X.; Pichler, M.; Allegrini, M.; Fioretti, A.; Comparat, D.; Pillet, P. *Phys. Rev. A* **2009**, *80*, 051401.
(10) Alessandro, M. D. *Introduction to Quantum Control and Dynamics*; Chapman Hall: Boca Raton, FL, 2007.
(11) Weinstein, J. D.; deCarvalho, R.; Guillet, T.; Friedrich, B.; Doyle, J. M. *Nature* **1998**, *395*, 148.
(12) Toennies, J. P.; Vilesov, A. F. *Annu. Rev. Phys. Chem.* **1998**, *49*, 1.
(13) Toennies, J. P.; Vilesov, A. F. *Angew. Chem., Int. Ed.* **2004**, *43*, 2622.
(14) Auböck, G.; Aymar, M.; Dulieu, O.; Ernst, W. E. *J. Chem. Phys.* **2010**, *132*, 054304.
(15) Moroshkin, P.; Hofer, A.; Lebedev, V.; Weis, A. *J. Chem. Phys.* **2010**, *133*, 174510.
(16) Li, D.; Xie, F.; Li, L.; Magnier, S.; Sovkov, V. B.; Ivanov, V. S. *Chem. Phys. Lett.* **2007**, *441*, 39.
(17) Bünermann, O.; Mudrich, M.; Weidemüller, M.; Stienkemeier, F. *J. Chem. Phys.* **2004**, *121*, 8880.
(18) Ernst, W. E.; Huber, R.; Jiang, S.; Beuc, R.; Movre, M.; Pichler, G. *J. Chem. Phys.* **2006**, *124*, 024313.
(19) DeMille, D.; Sainis, S.; Sage, J.; Bergeman, T.; Kotochigova, S.; Tiesinga, E. *Phys. Rev. Lett.* **2008**, *100*, 043202.
(20) Bovino, S.; Coccia, E.; Bodo, E.; López-Durán, D.; Gianturco, F. A. *J. Chem. Phys.* **2009**, *130*, 224903.
(21) Prosmiti, R.; Delgado-Barrio, G.; Villarreal, P.; Yurtsever, E.; Coccia, E.; Gianturco, F. A. *J. Phys. Chem. A* **2009**, *113*, 14718.
(22) López-Durán, D.; de Lara-Castells, M. P.; Delgado-Barrio, G.; Villarreal, P.; Di Paola, C.; Gianturco, F. A.; Jellinek, J. *Phys. Rev. Lett.* **2004**, *93*, 053401.
(23) Villarreal, P.; Roncero, O.; Delgado-Barrio, G. *J. Chem. Phys.* **1994**, *101*, 2217.
(24) Hernández, M. I.; Halberstadt, N.; Sands, W. D.; Janda, K. C. *J. Chem. Phys.* **2000**, *113*, 7252.
(25) Roncero, O.; Pérez-de Tudela, R.; de Lara-Castells, M. P.; Prosmiti, R.; Delgado-Barrio, G.; Villarreal, P. *Int. J. Quantum Chem.* **2007**, *107*, 2756.
(26) Roncero, O.; de Lara-Castells, M. P.; Delgado-Barrio, G.; Villarreal, P.; Stoecklin, T.; Voronin, A.; Rayez, J. C. *J. Chem. Phys.* **2008**, *128*, 164313.
(27) Wernli, M.; Bodo, E.; Gianturco, F. A. *Eur. Phys. J. D* **2007**, *45*, 267.
(28) Linear Algebra Package 3.2.1. 2009; http://www.netlib.org/lapack/
(29) Márquez-Mijares, M.; de Tudela, R. P.; González-Lezana, T.; Roncero, O.; Miret-Artés, S.; Delgado-Barrio, G.; Villarreal, P.; Baccarelli, I.; Gianturco, F. A.; Rubayo-Soneira, J. *J. Chem. Phys.* **2009**, *130*, 154301.
(30) Di Paola, C.; Gianturco, F. A.; López-Durán, D.; de Lara-Castells, M. P.; Delgado-Barrio, G.; Villarreal, P.; Jellinek, J. *ChemPhysChem* **2005**, *6*, 1348.
(31) Coccia, E.; Gianturco, F. A. *J. Phys. Chem. A* **2010**, *114*, 3221.
(32) Bodo, E.; Coccia, E.; López-Durán, D.; Gianturco, F. A. *Phys. Scr.* **2007**, *76*, C104.
(33) Lewerenz, M. *J. Chem. Phys.* **1997**, *106*, 4596.
(34) Guardiola, R.; Navarro, J. *Phys. Rev. A* **2006**, *74*, 025101.
(35) Ceperley, D. M. *Rev. Mod. Phys.* **1995**, *67*, 279.
(36) Bose, A. *J. Math. Phys.* **1989**, *30*, 2035.
(37) Brualla, L.; Sakkos, K.; Boronat, J.; Casulleras, J. *J. Chem. Phys.* **2004**, *121*, 636.
(38) Sakkos, K.; Casulleras, J.; Boronat, J. *J. Chem. Phys.* **2009**, *130*, 204109.
(39) Cao, J.; Berne, B. J. *J. Chem. Phys.* **1989**, *91*, 6359.
(40) Herman, M. F.; Bruskin, E. J.; Berne, B. J. *J. Chem. Phys.* **1982**, *76*, 5150.
(41) Barker, J. A. *J. Chem. Phys.* **1979**, *70*, 2914.
(42) Borrmann, P. *Comput. Mater. Sci.* **1994**, *2*, 593.
(43) Svensson, E. C.; Sears, V. F.; Woods, A. D. B.; Martel, P. *Phys. Rev. B* **1980**, *21*, 3638.
(44) Robkoff, H. N.; Hallock, R. B. *Phys. Rev. B* **1981**, *24*, 159.
(45) Bäck, T.; Schwefel, H.-P. *Evolut. Comput.* **1993**, *1*, 1.
(46) Iwamatsu, M. *Comput. Phys. Commun.* **2001**, *142*, 214–218.
(47) Valdés, A.; Prosmiti, R.; Villarreal, P.; Delgado-Barrio, G. *J. Chem. Phys.* **2005**, *122*, 044305.
(48) Valdés, A.; Prosmiti, R.; Villarreal, P.; Delgado-Barrio, G. *J. Chem. Phys.* **2006**, *125*, 014313.
(49) Tang, K. T.; Toennies, J. P. *J. Chem. Phys.* **2003**, *118*, 4976.
(50) Janzen, A. R.; Aziz, R. A. *J. Chem. Phys.* **1995**, *103*, 9626.
(51) González-Lezana, T.; Rubayo-Soneira, J.; Miret-Artés, S.; Gianturco, F. A.; Delgado-Barrio, G.; Villarreal, P. *Phys. Rev. Lett.* **1999**, *82*, 1648.

(52) Coccia, E.; Bodo, E.; Gianturco, F. A. *J. Chem. Phys.* **2009**, *130*, 094906.
(53) Sprik, M.; Klein, M. L.; Chandler, D. *Phys. Rev. B* **1985**, *31*, 4234.
(54) Metropolis, N.; Rosenbluth, A. W.; Rosenbluth, M. N.; Teller, A. H.; Teller, E. *J. Chem. Phys.* **1953**, *21*, 1087.
(55) Warnecke, S.; Sevryuk, M. B.; Ceperley, D. M.; Toennies, J. P.; Guardiola, R.; Navarro, J. *Eur. Phys. J. D* **2010**, *56*, 353.
(56) Zillich, R. E.; Whaley, K. B. *J. Phys. Chem. A* **2007**, *111*, 7489.
(57) López-Durán, D.; de Tudela, R. P.; Rodrguez-Cantano, R.; González-Lezana, T.; Delgado-Barrio, G.; Villarreal, P. *Phys. Scr.* **2011**, in press.
(58) Boronat, J.; Sakkos, K.; Sola, E.; Casulleras, J. *J. Low Temp. Phys.* **2007**, *148*, 845.
(59) de Lara-Castells, M. P.; Prosmiti, R.; López-Durán, D.; Delgado-Barrio, G.; Villarreal, P.; Gianturco, F. A.; Jellinek, J. *Int. J. Quantum Chem.* **2007**, *107*, 2902.
(60) (a) López-Durán, D.; de Lara-Castells, M. P.; Delgado-Barrio, G.; Villarreal, P.; Di Paola, C.; Gianturco, F. A.; Jellinek, J. *J. Chem. Phys.* **2004**, *121*, 2975. (b) de Lara-Castells, M. P.; López-Durán, D.; Delgado-Barrio, G.; Villarreal, P.; Di Paola, C.; Gianturco, F. A.; Jellinek, J. *Phys. Rev. A* **2005**, *71*, 033203. (c) de Lara-Castells, M. P.; Prosmiti, R.; Delgado-Barrio, G.; López-Durán, D.; Villarreal, P.; Gianturco, F. A.; Jellinek, J. *Phys. Rev. A* **2006**, *74*, 053201. (d) Villarreal, P.; de Lara-Castells, M. P.; Prosmiti, R.; Delgado-Barrio, G.; López-Durán, D.; Gianturco, F. A.; Jellinek, J. *Phys. Scr.* **2007**, *76*, C96.
(61) Felker, P. M. *J. Chem. Phys.* **2006**, *125*, 184313.
(62) (a) de Lara-Castells, M. P.; Delgado-Barrio, G.; Villarreal, P.; Mitrushchenkov, A. O. *J. Chem. Phys.* **2006**, *125*, 221101. (b) de Lara-Castells, M. P.; Mitrushchenkov, A. O.; Delgado-Barrio, G.; Villarreal, P. *Few-Body Syst* **2009**, *45*, 233. (c) de Lara-Castells, M. P.; Villarreal, P.; Delgado-Barrio, G.; Mitrushchenkov, A. O. *J. Chem. Phys.* **2009**, *131*, 194101. (d) de Lara-Castells, M. P.; Aguirre, N. F.; Villarreal, P.; Delgado-Barrio, G.; Mitrushchenkov, A. O. *J. Chem. Phys.* **2010**, *132*, 194313. (e) de Lara-Castells, M. P.; Villarreal, P.; Delgado-Barrio, G.; Mitrushchenkov, A. O. *Int. J. Quantum Chem.* **2011**, *111*, 406.